13

Sputum Smear Microscopy for Tuberculosis: Evaluation of Autofocus Functions and Automatic Identification of Tuberculosis Mycobacterium

Cicero F. F. Costa Filho and Marly G. F. Costa
Centre for Electronic and Information Technology/Federal University of Amazonas
Brazil

1. Introduction

Since 1997 the World Health Organization has published an annual report on global control of tuberculosis (TB) with the purpose of providing a comprehensive and up-to-date assessment of the TB epidemic. According to the Global TB control report of 2010 (World Health Organization [WHO], 2010), the global burden of disease caused by TB in 2009 is as follows: 9.4 million incident cases, 14 million prevalent cases, 1.3 million deaths among non HIV-positive people and 0.38 million deaths among HIV positive people.

The absolute number of cases continues to increase from year to year. The slow reduction in incident rates per capita is outweighed by increases in population. The greatest number of cases are in Asia (55%) and Africa (30%). Other regions have lower numbers of cases: Eastern Mediterranean Region (7%), European Region (4%) and American Region (3%). The main effort of WHO today concerning TB is to attain the targets included in the Millennium Development Goals (MDGs).

Adopted by world leaders in 2000, the MDGs are a blueprint that guides the efforts of the United Nations Development Program and various and various aid agencies, providing concrete, numerical benchmarks for tackling extreme poverty in its many dimensions to be achieved by 2015. The MDGs define 8 goals (United Nations [UN], 2010) with 21 targets that are measured by 60 indicators. TB falls under the 6th goal related to fighting disease epidemics, aiming to: "Combat HIV/AIDS, Malaria and other diseases". Within this goal the following target refers to TB: "Halt and begin to reverse the incidence of malaria and other major diseases". Related to this target, the following indicator refers to TB: Halt and begin to reverse TB incidence by 2015; Reduce prevalence and deaths due to TB by 50% compared with a baseline of 1990.

To achieve these indicators the WHO adopted a Partnership Global Plan to Stop TB (WHO, 2011). Launched in January 2006, it includes sputum smear microscopy as the main diagnostic tool. Indeed, one of the targets of this plan is stated as follows: "A treatment success rate among sputum smear positive case of 90%". The main reason for sputum smear

microscopy to be included is that it is the main non-invasive technique employed for TB diagnosis. Other non-invasive techniques include culture and chest radiography.

Sputum smear microscopy has several operational advantages over culture as a diagnostic tool (Luelmo, 2004): "The results are available soon, correlate with infectiousness, and identify both patients at high risk of death from tuberculosis if untreated and patients who require more drugs in the initial treatment regimen because of greater bacterial load". In addition sputum smear microscopy has an important role in follow up of TB treatment. Only when the smears are negative can the intensive phase of the treatment be suspended.

Despite the historical importance of chest radiography in TB diagnosis, it is not used today as a diagnostic tool alone. The following reasons justify this practice: 1) Some other diseases of the lung show a similar appearance in radiographic picture. Consequently radiographic exam is not specific to TB; 2) Lesions of pulmonary tuberculosis can take almost any form in a radiographic image (American Thoracic Society [ATS], 2000) .

Two main facts enable the use of sputum smear microscopy for TB diagnosis. The first one is that special dyes allow to differentiating the bacillus from the background. The second one is that there is a positive correlation between the number of bacillus in the smear and the probability of their being identified by microscopy.

To support the last statement, Table 1 (David, 1976, as cited in Toman, 2004a) shows the positive correlation that exists between the number of bacillus present in a sputum specimen, the number of bacillus in a smear and the probability of finding theses bacillus by microscopy. For this study 0.01 ml of sputum was placed on a slide and spread over an area of 200mm^2. The magnification of the microscope used allowed for observing 10.000 fields on this slide.

No. of bacilli observed	Estimated concentration of bacilli per ml of especimen	Probability of a positive result
0 in 100 or more field	<1000	<10%
1-2 in 300 fields	5000-10000	50%
1-9 in 100 fields	about 30 000	80%
1-9 in 10 fields	about 50 000	90%
1-9 per field	about 100 000	96.2%
10 or more per field	about 500 000	99.95%

Table 1. Number of observed bacilli, concentration of bacilli in sputum specimen (culture results) and probability of a positive result

Two techniques are used for TB diagnostic with sputum smear microscopy: Fluorescence microscopy and conventional microscopy. Fluorescence microscopy uses an acid-fast fluorochrome dye (eg, auramine O or auramine-rhodamine), while conventional microscopy uses the carbolfuchsin Ziehl-Neelsen - ZN or Kinyoun acid-fast stains. While the first one uses an intense light source, such as a halogen or high-pressure mercury vapor lamp, the second one uses a conventional artificial light source.

1. Fluorescence microscopy has the following main advantages over conventional microscopy: 1) Fluorescence microscopy uses a lower power objective lens (typically 25x), while conventional microscopy uses a higher power objective lens (typically 100x). As a consequence fluorescence microscopy allows the same area of a smear to be scanned in a much shorter time than with conventional microscopy (Bennedesen & Larsen, 1966);
2. Fluorescence microscopy is on average 10% more sensitive than conventional microscopy (Steingart et. al., 2006).

The main shortcomings of fluorescence microscopy are: 1) The relatively high costs of the microscopy unit and its maintenance when compared with the conventional microscopy unit; 2) The handling and maintenance of the optical equipment require advanced technical skill (Toman, 2004b).

The sensitivity of tuberculosis diagnostic through sputum smear analysis reported in the literature varies greatly. While reported sensitivities of conventional microscopy range from 0.32 to 0.94, reported sensitivities of fluorescence microscopy range from 0.52 to 0.97. On average the specificity of fluorescence microscopy is similar to conventional microscopy and range from 0.94 to 1 (Steingart et. al., 2006).

In addition to the huge variability in sensitivity, the manual screening for bacillus identification is a labor-intensive task that consumes between 40 minutes and 3 hours, depending on patient's level of infection and it is needed to analyse 40-100 images (Sotaquirá, 2009).

Automatic methods for bacilli screening were first developed for fluorescence microscopy images (Veropoulos et. al., 1998; Forero et. al., 2003). The first methods for automatic bacilli screening in conventional microscopy were published only in 2008 (Costa et. al., 2008; Sadaphal et. al., 2008; Raof et. al., 2008). Some other methods for automatic bacilli screening were published in recent years (Forero, 2004, 2006; Lenseigne et. al., 2007; Sotaquira et. al., 2009; Makkapati, et. al., 2009; Khutlang et. al., 2010).

Some authors (Forero et. al., 2006; Sotaquira, 2009; Khutlang, 2010) claimed that the main advantages of an automatic bacilli screening over a manual one are better reproducible values for sensitivity and specificity and a faster screening process. Table 2 shows reported values for sensitivity, specificity and time waste for one image analysis using automatic methods.

The sensitivity and specificity values previously cited for manual screening methods refer to tuberculosis diagnosis. The sensitivity and specificity values for automatic methods shown in Table 2 refer to object classification as bacillus or not bacillus. Therefore, a rigorous comparison of sensitivities and specificities between manual and automatic screening methods could not be done.

Only one paper of Table 2 cited time wasted for one image analysis, 1.87s. To compute the time consumed with a TB automatic diagnosis it is necessary to take into account the number of images needed to achieve a correct diagnosis. As previously cited, in order to achieve a correct diagnosis, it is necessary to analyze between 20 and 100 fields of one slide. With an automatic procedure, it is also necessary to take into account the time spent with focusing computations, image acquisition and microscopy displacement. According to

Santos (Santos et. al., 1997) focusing computations takes 1.8s per field, while acquisition takes 0.7s, including 0.5s for slide movement. Assuming that no parallel process occurs and considering the worst case scenario of 100 images we have the time spent with an automatic diagnosis (T_{ad}) given by:

$$T_{ad} = 100x(1.87 + 1.8 + 0.7) = 437\text{s} \cong 7\ minutes \quad (1)$$

This value is a few times smaller than the value of 40 minutes previously cited for a TB manual diagnostic with sputum smear microscopy.

Author	Microscopy	Sensitivity (%)	Specificity (%)	Time for one image analysis (seconds)	Computer
Veropoulos, 1998	Fluorescence	93.53	98.79	not cited	--
Forero, 2006	Fluorescence	97.89	94.67	not cited	--
Sotaquira, 2009	Conventional	90.90	100	1.87	Intel processor of 2 GHz and 512 MB of RAM
Khutlang, 2010	Conventional	97.77	99.13	not cited	--

Table 2. Sensitivity, Specificity and time for one image analysis

Steps involved in automated microscopy include those shown if Figure 2. In the following sections, we analyze some of these steps. In section 2 we address the problem of auto focusing, discussing the main functions used in auto focusing methods. In the third section we discuss the main differences between the methods used for bacilli segmentation and classification in fluorescence microscopy and conventional microscopy.

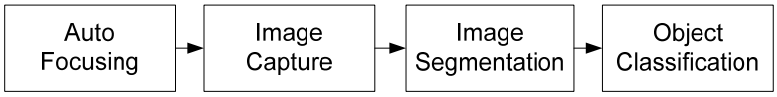

Fig. 2. Steps involved in automated bacilli recognition

2. Autofocus evaluation functions

Automatic microscopy is accomplished through coupling an electronic camera to a microscope. Auto focusing of electronic cameras is accomplished by searching for the lens position that gives the best focused image (Subbaro &. Tyan, 1995). A focused image can be thought of as one that, for a set of images captured with different microscope stages, presents the best average focus over an entire field of view. In a frequency viewpoint, a focused image can be thought of as one that has more high frequency components. It is important that samples be well prepared, resulting in thin structures, because thick samples present structures with different foci. An auto focusing process employs a focus measure and a procedure to determine the best focused image. A focus measure can be defined as follow: "First, the image for which the focus measure needs to be computed is normalized for brightness by dividing the image by its mean brightness. Then, it is convolved with a focus measure filter (FMF). Then, the energy (sum of squared values) of the filtered image is computed. This energy is the focus measure" (Subbaro &. Tyan, 1998). An important conclusion concerning focus measures, established by the same authors, is that the best focus measure could be different for different objects depending on both image content and

noise characteristic. In other words, there is no best focus measure that can be used for auto focusing of different image types. Because of this, it is important to find the best focus measure that can be used in TB auto focusing. In this section we will revise the main focus measure functions used in automatic microscopy.

The main focus measures functions used in auto focusing can be divided into four groups:

Functions Based on Image Differentiation

Different FMF have been used for image differentiation:

Threshold Absolute Gradient: This function computes and accumulates the first difference between a pixel and its neighbor with a distance of one, when the difference is larger than a threshold.

$$F_{th\_grad} = \sum_M \sum_N |g(i,j+1) - g(i,j)| \quad (2)$$

$$while\ |g(i,j+1) - g(i,j)| \geq \theta$$

Squared Gradient: Similar to the previous function but with squared difference. The larger differences influence the results more.

$$F_{sq\_grad} = \sum_M \sum_N |g(i,j+1) - g(i,j)|^2 \quad (3)$$

$$while\ |g(i,j+1) - g(i,j)| \geq \theta$$

Tenenbaum Gradient (Krotkov, 1987): This function uses the Sobel operator.

$$F_{tenen} = \sum_M \sum_N T[g(i,j)] \quad (4)$$

$$T[g(i,j)] = G_x^2(i,j) + G_y^2(i,j)$$

$$G_x(i,j), G_y(i,j) = Image\ convolution\ with\ Sobel\ operators$$

Brenner Gradient (Brenner et. al., 1971): This function computes the first difference between a pixel and its neighbor with a distance of two.

$$F_{brenner} = \sum_M \sum_N |g(i,j+2) - g(i,j)|^2 \quad (5)$$

$$while\ |g(i,j+1) - g(i,j)| \geq \theta$$

Energy of Image Laplacian: This function implements the image convolution with a Laplace mask.

$$F_{Laplace} = \sum_M \sum_N \left(g(i,j+1) + g(i,j-1) + g(i+1,j) + g(i-1,j) - 4g(i,j)\right)^2 \quad (6)$$

First order Gaussian Derivative (Geusebroeck et. al., 2000): This function involves image convolution with the derivative of a Gaussian smooth filter.

$$F_{Gaussian} = \frac{1}{NM} \sum_N \sum_M \left(g(i,j) * G_x(x,y,\sigma)\right)^2 + \left(g(i,j) * G_y(x,y,\sigma)\right)^2$$

$$G_x(x,y,\sigma)\ and\ G_y(x,y,\sigma)\ are\ the\ first\ order\ Gassuain\ derivatives\ in\ the\ x\ and\ y\ directions$$

$$\sigma\ is\ the\ standard\ deviation\ \cong\ (d/2)/\sqrt{3},\ \text{d= bacillus width}$$

Statistics-Based Functions

These functions evaluate the contrast of an image:

Variance: This function measures the variation in image gray level of pixels.

$$F_{var} = \frac{1}{MN}\sum_M \sum_N |g(i,j) - \bar{g}| \tag{7}$$

Normalized Variance: This function compensates for the differences in bright levels among different images

$$F_{var} = \frac{1}{MN\bar{g}}\sum_M \sum_N |g(i,j) - \bar{g}| \tag{8}$$

Functions Based on Histogram

Entropy: The entropy function is a measure of information content

$$F_{entr} = -\sum_l p_l log p_l \tag{9}$$

$$p_l \; is \; the \; relative \; frequency \; of \; gray \; level \; l$$

Variance of Log Histogram: This function emphasizes the bright pixels in the image by multiplying the variance by the logarithm

$$F_{var\_log} = \sum_l \big(l - \; E_{log}\{l\}\big) log p_l \tag{10}$$

$$E_{log}\{l\} = \sum_l l log p_l \; is \; the \; expected \; value \; of \; \log histogram$$

Functions Based on Correlation Measurement

These functions were proposed by Vollath (Vollath, 1998) and, according to the author, had good performance in noise presence.

Autocorrelation (Vollath's F_4):

$$F_{autocorr} = \sum_M \sum_N g(i+1,j)g(i,j) \; - \sum_M \sum_N g(i+2,j)g(i,j) \tag{11}$$

Standard Deviation-Based Correlation (Vollath's F_5):

$$F_{autocorr} = \sum_M \sum_N g(i+1,j)g(i,j) \; - MN\bar{g}^2 \tag{12}$$

Some measures based on frequency content have been proposed, such as the wavelet transform (Kautsky et. al., 2002). Nevertheless it did not present good results in TB auto focusing.

It should be observed that some of these functions depend on threshold, while some others do not depend on any parameter. Some of these functions were used for TB auto focusing. Table 3 shows published papers involving TB auto focusing, detailing the focus measure employed in each one.

The papers of Russel (Russel & Douglas, 2007) and Kimura (Kimura Junior et. al., 2010) were careful to consider slides with different background contents. For example, Kimura divided

the TB conventional microscopy images into two groups: Images with high density background content and images with low density background content. Figure 3(a) shows an image with high density background content and Figure 3(b) an image with low density background content. In both groups the variance and normalized variance functions showed the best performance. Osibote (Osibote et. al., 2010) also obtained a better performance with the normalized variance function.

Authors	Microscopy Type	Evaluation Functions	Results
Forero et. al. (2004)	Fluorescence	Variance, Energy of Image Laplacian, Wavelet Transform, Autocorrelation, Variance of Log Histogram	The best results were obtained with Variance of Log Histogram Function. Other measure produced meaningful results
Russel & Douglas (2007)	Conventional	Energy of Image Laplacian, First Order Gaussian Derivative, Variance of Log Histogram	The best results were obtained with Energy Laplacian Function. Compared with manual focus: average difference = 1.45μm. Standard deviation = 1.88μm.
Kimura Junior et. al. (2010)	Conventional	Brenner Gradient, Energy of Image Laplacian, Wavelet Transform, Variance, Normalized Variance, Autocorrelation, Standard Deviation-Based Correlation, Entropy, Variance of Log Histogram	The best results were obtained with Variance and Normalized Variance. Entropy was the quickest function. Wavelet function was the slower function.
Osibote et. al. (2010)	Conventional	Normalized Variance, Brenner Gradient, Energy of Image Laplacian, Autocorrelation, Tenembaum Gradient	The best results were obtained with Normalized Variance Function

Table 3. Published papers involving TB auto focusing

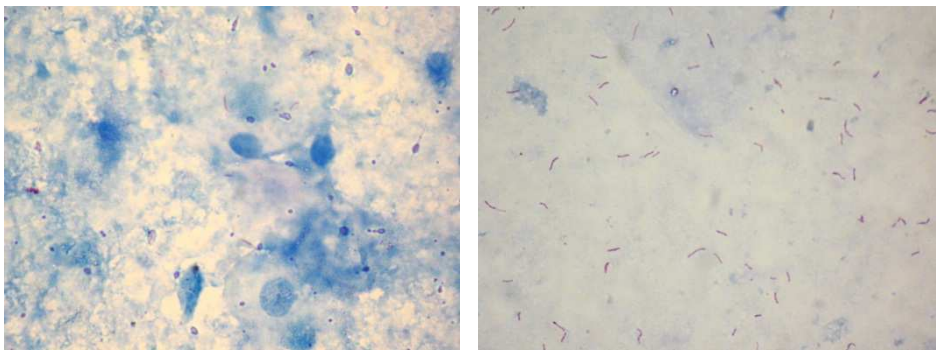

(a) (b)

Fig. 3. Images with different density background content. (a) high density background content; (b) low density background content

The shape of a focus function typically resembles a Gaussian curve as shown if Figure 4.

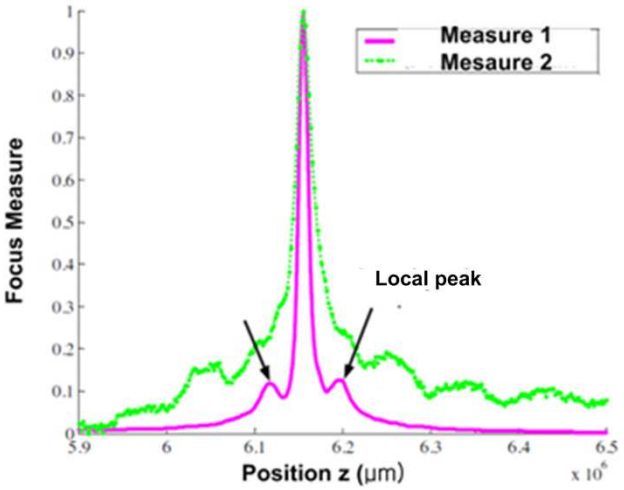

Fig. 4. Typical shape of a focus function

The horizontal coordinate of the graph of Figure 4 corresponds to the z position of the microscope vertical axis. To plot the focus function it is necessary to vary this z position and obtain a stack of points described in equation (13). The z position movement for obtaining the image stack is illustrated in Figure 5.

$$\text{Stack} = \{(FM_1, z_1), (FM_2,z_2),\ldots\ldots..(FM_{n/2}z_{n/2})\ldots.(FM_{n-1}z_{n-1})\ (FM_n,z_n)\} \quad (13)$$

Where: FM_i = Focus measure at position z_i

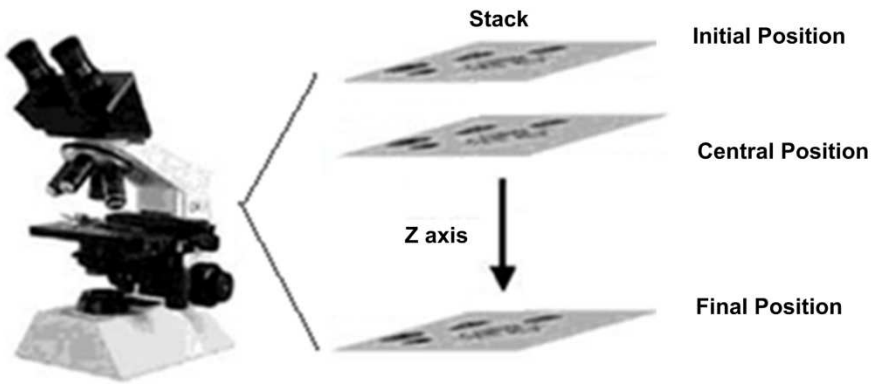

Fig. 5. Z position movement for obtaining the image stack

The in-focus image normally is the central image of the stack. Varying the z position changes the image sharpness and hence the degree of focus. Each image in a stack, therefore, is at a different focus level. For focus measure computation, images are converted from RGB

to gray scale. The performance of a focus measure is frequently evaluated using the focus curve and according to four features (Firestone at. al., 1991), defined as:

1. Accuracy: expressed here as the number of steps by which the maximum of a particular focus function departs from the correct focal position;

Range: the number of steps between the two neighboring local minima around the global maximum;

Number of false maxima: number of spurious focus function maxima;

Width: computed at 50% of the height focus curve. This criterion describes the sharpness or narrowness of the peak.

Santos et al. (1997) introduced a 5th feature, Execution Time, as follows:

Execution Time: the time taken for an algorithm to compute the focus plot and locate the position of maximum focus.

According to Santos (Santos et. al., 1997) a quantitative evaluation may compare a focus curve to an ideal function with respect to each of these features. The authors define an ideal focus function as having a value of 0 for execution time, accuracy, width and number of false maxima and a range determined by multiplying the number of images in the stack used to plot the focus function and the step size between each position in the stack (adjustment step of the microscopy). To obtain a measure of how a focus measure departs from an ideal behavior the following algorithm is used:

1. A series of focus measure curves is obtained (these series should contain images with different background content). The mean and the standard deviation of each feature in the series are obtained.
2. The five feature values of each image series are normalized by subtracting the corresponding mean and dividing by the standard deviation. This produces values for the different features that can be compared as they all now have mean zero and standard deviation equal to unity.
3. For each feature the distance from the ideal function is computed. First the differences between the feature value in the function and in the ideal function are obtained. Then the square root of the addition of the squares of these results is computed.
4. Finally, to produce a final figure of this function, the mean value of the five distances is obtained.

When doing a TB diagnosis with sputum smear microscopy, a bacilli count on a number of fields of one slide is necessary. A time-consuming autofocus procedure determines the optimal focus through the acquisition of the focus function for each field. To reduce lens motion and achieve faster autofocus times the following procedure proposed by Osibote (Osibote et. al., 2010) can be used:

1. Obtaining the focus position for the first field of the slide through the acquisition of a full image stack of the focus measure, ensuring a perfect evaluation of this field to avoid locating the optimal focus in a false minimum position;
2. Adopt a simplified procedure to determine the optimal focus position in subsequent fields, using the optimal focus position of the previous field as a reference. For this purpose the procedure proposed by Yanzdafar (Yanzdafar et. al., 2008) can be used.

3. Automated sputum smear microscopy

According to Forero (Forero et. al., 2006) bacilli are structures that have a length between 1 and 10 μm and a width between 0.2 and 0.6 μm presenting a straight, curve or bent shape, as shown if Figure 6.

Fig. 6. Different shapes of bacilli

Depending on the staining procedures used, the bacilli assume different appearances. When the sputum smear is stained with an acid-fast fluorochrome dye, as is the case when fluorescence microscopy is used, the bacilli fluoresce in the range between green and yellow up to white, while the background is dark. Otherwise, when the sputum smear is stained with carbolfuchsin Ziehl-Neelsen - ZN or Kinyoun acid-fast stains, as is the case when conventional microscopy is used, the bacilli may have different colours, varying from light fuchsia to dark purple. In Figure 7 we show images of both microscopy types.

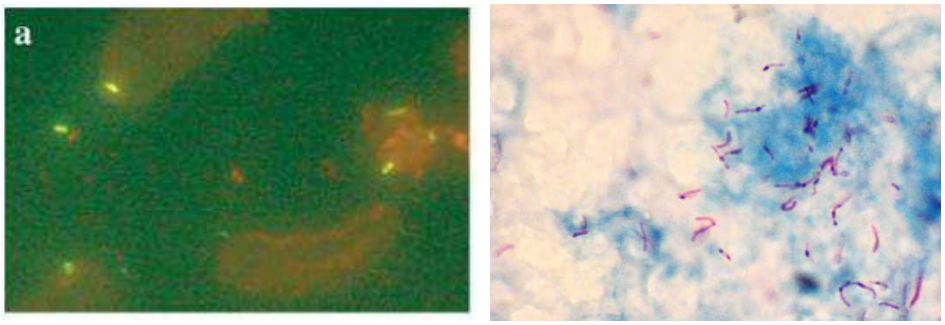

Fig. 7. Fluorescence microscopy (after Forero et al., 2004) and conventional microscopy sputum smear image

The block diagram of Figure 2 shows the main steps involved in automated bacilli recognition. Table 4 shows the main methods used in the literature for each step of this block diagram.

As shown in Figure 2, after image capture, bacilli segmentation is performed. The segmentation procedures adopted in both types of images shown in Figure 7 are completely different from each other.

In fluorescence microscopy images, the bacilli are easily separated from the background with a threshold operation. Afterwards, the segmentation is performed using edge detection

operators, such as canny operators (Veropoulos et. al., 1998; Forero et. al., 2004). Intermediate steps for edge linking and boundary tracing are also employed. Figure 8 shows the results of the segmentation procedure used by Forero (Forero et. al., 2004) when applied to the image on the left side of Figure 7.

In conventional microscopy images, the bacilli are not easily separated from the background with a threshold operation. In this case, for bacilli segmentation, colour space techniques are used. As shown in Table 4, the techniques found in the literature vary: histogram based techniques, Bayesian pixel classifiers, KNN pixel classifiers, etc. The colour spaces used also vary: RGB, YCbCr and Lab

Author	Microscopy	Bacilli segmentation	Bacilli Classification	Results
Veropoulos et. al, 1998	Fluorescence	Edge detection techniques: Canny operator	**Shape Descriptors:** 15 Fourier descriptors; **Classifier:** Back-propagation (BP), RBF networks, KNN, Kernel Regression (KR)	**Accuracy:** BP - 97.57% RBF - 88.06% KNN - 91.80 KR - 95.24%
Forero et. al, 2004	Fluorescence	Edge detection techniques (Canny operator) + Adaptive color thresholding (RGB color space)	**Shape Descriptors:** compactness, eccentricity and Hu's moments descriptors; **Classifier:** Classification tree	**Specificity, Sensitivity:** 99.74%, 73.33% 94.96%, 86.66%
Forero et. al, 2006	Fluorescence	Edge detection techniques (Canny operator) + Adaptive color thresholding	**Shape Descriptors:** Hu's moments descriptors; **Classifier:** Gaussian mixture models	**Specificity, Sensitivity:** 97.89%, 94.67% 98.10%, 92.9%
Costa et. al., 2008	Conventional	**Color space techniques:** Adaptive global threshold; **Color space:** RGB	Size filters	**Sensitivity:** 76.65% **False Positive Rate:** 12%
Sadaphal et. al., 2008	Conventional	**Color space techniques:** Bayesian segmentation; **Color space:** RGB	**Shape Descriptors:** Axis ratio, eccentricity; **Classifier:** Classification tree	No information
Raof et. al., 2008	Conventional	**Color space techniques:** Thresholding; **Color space:** RGB		No information
Sotaquirá et. al. , 2009	Conventional	**Color space techniques:** First derivative of histogram; **Color space:** YCbCr, Lab		**Accuracy:** 96.3% **False detection:** 9.78%
Khutlang et. al. (2010)	Coventional	**Color space techniques:** Pixel classifiers (Baye's, Linear regression, quadratic discriminant); **Color space:** RGB	**Shape Descriptors:** Fourier features, color moments, eccentricity, compactness; **Classifier:** Probabilistic neural network, kNN, SVM	**Accuracy:** 98.55% **Sensitivity:** 97.77% **Specificity:** 99.13%

Table 4. Published papers involving Automated Sputum Smear Microscopy

After the segmentation step is finished, not only bacilli are segmented. Some structures fluoresce the same way as bacilli in fluorescence microscopy images. Similarly some structures have the same colour properties as bacilli in conventional microscopy images. confused with bacilli. These structures, also called noise, could be debris or cells present in the background. To illustrate this point, near the lower left corner of Figure 7, a circular structure can be seen that fluoresces the same way as a bacillus, but because of its circular shape could not be classified as one. Nevertheless, this structure is segmented the same way as a bacillus, as shown in Figure 8.

Fig. 8. Objects resulting from segmentation procedures applied in the left image of Figure 7.

To separate noise from bacilli in the segmented images an additional step, called object classification in the block diagram of Figure 2 is normally employed. For this purpose classifiers using shape descriptors are used. As the bacilli may have different sizes, positions and orientations, the shape descriptors used must be rotation, translation and scale invariant. As shown in Table 4, the most used descriptors used are: compactness, eccentricity, Hu's moments and Fourier Descriptors. Varied classifiers such as classification trees, Support Vector Machines and Neural Networks were employed by some authors in order to recognize the bacilli.

The results presented in Table 4 show that, in bacilli detection, results for sensitivity and specificity as good as 97.77% and 99.13% are cited. It is noteworthy, however that the authors who cited these values, do not consider touching bacilli. In some cases, as the one shown in Figure 9, these bacilli are present in large quantities. Disregarding these bacilli implies a different count of what is done by manual means. Because of this, we believe that other ways of removing noise than those that use shape descriptors must be investigated.

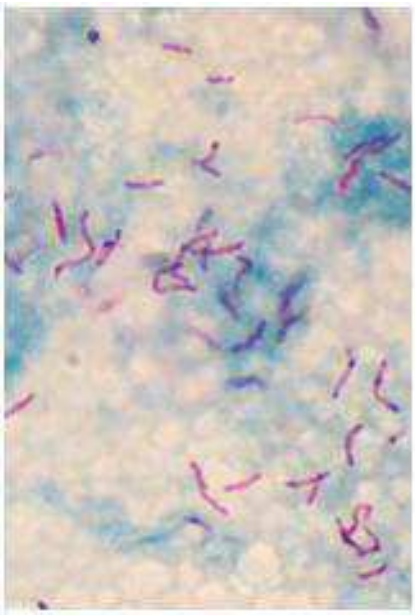

Fig. 9. Conventional microscopy image showing some examples of touching bacilli

4. References

ATS (2000). Diagnostic standards and classification of tuberculosis in adults and children. *American Journal of Respiratory and Critical Care Medicine*, Vol. 161, pp. 1376–1395, ISSN 1073-449X

Brenner, J.F., Dew, B.S., Horton, J.B., King, J.B., Netrath, P.W. & Sellers, W.B. (1971), An automated microscope for cytologic research, *Journal of Histochemistry and Cytochemistry*, Vol. 24, pp 100-111, ISSN 0022-1554

Bennedsen, J. & Larsen, S. O. (1966), Examination for tubercle bacilli by fluorescence, *Scandinavian Journal of Respiratory Disease*, Vol. 47, pp.114–20, ISSN 0036-5572

Costa, M. G. F., Costa Filho, C. F. F., Sena, J. F., Salen, J. & Lima, M. O. (2008), Automatic identification of mycobacterium tuberculosis with conventional light microscopy, *Proceedings of the 30th Annual International Conference of the IEEE EMBS*, pp. 382-385,Vancouver, British Columbia, Canada

Firestone, L., Cook, K., Culp, K., Talsania, N. & Preston Jr, K. (1991), Comparison of autofocus methods for automated microscopy, *Cytometry*, Vol. 12, pp.195-206

Forero, M. G. & Cristóbal, G. (2003), Automatic identification techniques of tuberculosis bacteria, *Proc. SPIE*, Vol. 5203, pp. 71–81, ISSN 0277-786X

Forero, M.G., Sroubek, F. & Cristóbal, G. (2004). Identification of tuberculosis bacteria based on shape and color, *Real Time Imaging*, Vol. 10, pp. 251–262, ISSN 1077-2014

Forero, M.G., Cristóbal, G. & Desco, M. (2006), Automatic identification of Mycobacterium tuberculosis by Gaussian mixture models, *Journal of Microscopy*, Vol. 223, pp. 120–132, ISSN 0022-2720

Geusebrock, J., Cornelissen, F., Smeulders, A.W.M. & Geerts, G. (2000), Robust auto focusing in microscopy, *Cytometry*, Vol. 39, pp.1-9, ISSN 0196-4763

Kautsky, J., Flusser, .J, Zitova, B. S. & Imberova, S., (2002), A new waveletbased measure of image focus. *Pattern Recognition Letters*, Vol. 23, pp. 1785–1794.

Khutlang, R., Krishnan, S., Dendere, R., Whitelaw, A., Veropoulos, K., Learmonth, G. & Douglas, T. S. (2010), Classification of Mycobacterium tuberculosis in Images of ZN-Stained Sputum Smears, *IEEE Transactions on Information Technology in Biomedicine*, Vol. 14, No. 4, pp. 949-957, ISSN 1089-7771

Kimura Junior, A., Costa, M., Costa Filho, C. F. F., Fujimoto, L. B.M. & Salem, J. (2010), Evaluation of autofocus functions of conventional sputum smear microscopy for tuberculosis, *32th Annual International IEEE EMBS Conference*, pp. 3041-3044

Krotkov, E. (1987), Focusing, *International Journal of Computer Vision*, Vol. 1, pp. 223-227, ISSN 0920-5691

Lenseigne, B., Brodin, P., Christophe, T. & Genovesio, A. (2007), Support vector machines for automatic detection of tuberculosis bacteria in confocal microscopy images, *Proceedings of 4th IEEE International Symposium on Biomedical Imaging*, pp. 85-88, ISBN 0-7803-7585-8, Arlington, VA, USA

Luelmo, F. (2004), What is the role of sputum microscopy in patients attending health facilities?, In: *Toman's Tuberculosis Case detection, treatment, and monitoring –questions and answers*, T. Frieden, pp. 7-10, World Health Organization, ISBN 9241546034, Hong Kong, China

Makkapati, V., Agrawal, R. & Acharya, R. (2009), Segmentation and Classification of Tuberculosis Bacilli from ZN-stained Sputum Smear Images, *Proceddings of 5th Annual IEEE Conference on Automation Science and Engineering*, pp. 217-220, ISBN 978-1-60566-750-8 , Bangalore, India

Osibote, O.A., Dendere, R., Krishnan, S. & Douglas, T.S. (2010), Automated focusing in bright-field microscopy for tuberculosis detection, *Journal of Microscopy*, Vol. 240, 2, pp.155-163, ISSN 0022-2720

Raof, R. A. A., Salleh, Z., Sahidan, S. I., Mashor, M. Y., Md Noor, S. S., Idris, F. M. & Hasan, H. (2008), Color Thresholding Method For Image Segmentation Algorithm of Ziehl-Neelsen Sputum Slide Images, *Proceedings of 5th International Conference on Electrical Engineering, Computing Science and Automatic Control*, pp. 212-217, ISBN 978-1-4244-2499-3, Mexico City, Mexico

Russel, M.J & Douglas, T. S. (2007), Evaluation of autofocus algorithms for tuberculosis microscopy, *29th Annual International IEEE EMBS Conference*, pp. 3489-3492

Sadaphal, P, Rao, J., Comstock, G.W. & Beg, M.F. (2008), Image processing techniques for identifying Mycobacterium tuberculosis in Ziehl-Neelsen stains. *International Journal of Tuberculosis Lung Disease,* Vol. 12, n. 5, pp. 579-582, ISSN 1027-3719.

Santos, A., Ortiz-Solorzano, C.; Vaquero, J.; Malpica, N.; Pozo, F. Del (1997), Evaluation of autofocus functions in molecular cytogenetic analysis. *Journal of Microscopy*, Vol. 188, pp. 264–272, ISSN 0022-2720

Sotaquirá, M., Rueda, L. & Narvaez, R. (2009), Detection and quantification of bacilli and clusters present in sputum smear samples: a novel algorithm for pulmonary tuberculosis diagnosis, *Proceedings of International Conference on Digital Image Processing*, pp. 117-121, ISBN 978-0-7695-3565-4 , Bankoc, Thailand

Steingart, K. R., Henry, M., Ng, V., Hopewell, P. C., Ramsay, A., Cunningham, J., Urbanczik, R., Perkins, M., Aziz, M. A. & Pai, M. (2006), Fluorescence versus conventional sputum smear microscopy for tuberculosis: a systematic review, *Lancet Infectious Deseases*, Vol. 6, pp. 570-581, ISSN 1473-3099

Subbarao, M. & Tyan, J. K. (1995), The Optimal Focus Measure for Passive Autofocusing and Depth-from-Focus, *Proc. SPIE Conf. Viedometrics IV*, Vol. 2, 598, pp. 89-99, Philadelphia, ISBN 0-8194-1321-6

Subbarao, M. & Tyan, J. K. (1998), Selecting the Optimal Focus Measure for Autofocusing and Depth-From-Focus, *IEEE Transactions on Pattern Analysis and Machine Intelligence*, Vol. 20, 8, pp. 864-870, ISSN 0162-8828

UN, The Millennium Development Goals Report 2010 (2010), 18/05/2011, Available from: <http://www.un.org/millenniumgoals/reports.shtml >

Toman, K. (2004a), How reliable is smear microscopy?, In: *Toman's Tuberculosis Case detection, treatment, and monitoring –questions and answers*, T. Frieden, pp. 7-10, World Health Organization, ISBN 9241546034, Hong Kong, China

Toman, K. (2004b), What are the advantages and disadvantages of fluorescence microscopy?, In: *Toman's Tuberculosis Case detection, treatment, and monitoring – questions and answers*, T. Frieden, pp. 7-10, World Health Organization, ISBN 9241546034, Hong Kong, China

Veropoulos, K., Campbell, C., Learmonth, G., Knight, B., & Simpson, J (1998), The Automated Identification of Tubercle Bacilli using Image Processing and Neural Computing Techniques, *Proceedings of 8th International Conference on Artificial Neural Networks*, Vol. 2, pp. 797-802, ISBN 3540762639 ,Skövde, Sweden,.

Vollath, D. (1988), The influence of the scene parameters and of noise on the behaviour of automatic focusing algorithms, *Journal of Microscopy,* Vol. 151, pp.133-146

WHO, Global TB Control report (2010). 18/05/2011, Available from: <http://www.who.int/tb/publications/global_report/2010/en/index.html >

Yazdanfar, S., Kenny, K.B., Tasimi, K., Corwin, A.D., Dixon, E.L. & Filkins R.J. (2008), Simple and robust image-based auto focusing for digital microscopy. *Optics Express*. Vol. 16, pp. 8670–8677.

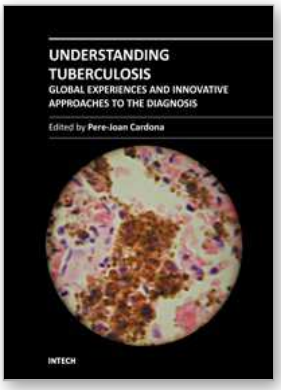

Understanding Tuberculosis - Global Experiences and Innovative Approaches to the Diagnosis

Edited by Dr. Pere-Joan Cardona

ISBN 978-953-307-938-7
Hard cover, 552 pages
Publisher InTech
Published online 15, February, 2012
Published in print edition February, 2012

Mycobacterium tuberculosis is a disease that is transmitted through aerosol. This is the reason why it is estimated that a third of humankind is already infected by Mycobacterium tuberculosis. The vast majority of the infected do not know about their status. Mycobacterium tuberculosis is a silent pathogen, causing no symptomatology at all during the infection. In addition, infected people cannot cause further infections. Unfortunately, an estimated 10 per cent of the infected population has the probability to develop the disease, making it very difficult to eradicate. Once in this stage, the bacilli can be transmitted to other persons and the development of clinical symptoms is very progressive. Therefore the diagnosis, especially the discrimination between infection and disease, is a real challenge. In this book, we present the experience of worldwide specialists on the diagnosis, along with its lights and shadows.

INTECH
open science | open minds

InTech Europe
University Campus STeP Ri
Slavka Krautzeka 83/A
51000 Rijeka, Croatia
Phone: +385 (51) 770 447
Fax: +385 (51) 686 166
www.intechopen.com

InTech China
Unit 405, Office Block, Hotel Equatorial Shanghai
No.65, Yan An Road (West), Shanghai, 200040, China
中国上海市延安西路65号上海国际贵都大饭店办公楼405单元
Phone: +86-21-62489820
Fax: +86-21-62489821